

## 采用稀释成盐法从富硼浓缩盐卤中合成的 镁硼酸盐化合物及其结构与性质

彭姣玉<sup>1,2,3</sup> 林 锋<sup>1,2,3</sup> 杨 波<sup>1</sup> 王立平<sup>1,2,3</sup> Dinnebier E. Robert<sup>4</sup> 董亚萍<sup>\*,1,2</sup> 李 武<sup>1</sup>

(<sup>1</sup> 中国科学院青海盐湖研究所, 西宁 810008)

(<sup>2</sup> 中国科学院大学, 北京 100049)

(<sup>3</sup> 中国科学院盐湖资源综合高效利用重点实验室, 西宁 810008)

(<sup>4</sup> 德国马克斯-普朗克固体研究所, 斯图加特 70569)

**摘要:** 通过稀释成盐法在富硼浓缩盐卤体系 Na-K-Mg-Cl-SO<sub>4</sub> 中合成了一种新的六硼酸镁 Mg[B<sub>6</sub>O<sub>7</sub>(OH)<sub>6</sub>]·5H<sub>2</sub>O 化合物。根据 X 射线粉末衍射数据对其晶体结构进行了精修, 并采用红外及拉曼光谱法对其结构进行了表征, 分析了其光谱及结构特征。结果表明, 该化合物由 1 个 Mg 原子、1 个 B<sub>6</sub>O<sub>7</sub>(OH)<sub>6</sub> 基团和 5 个 H<sub>2</sub>O 分子构成, Mg 原子以六配位形式与氧结合形成畸变 MgO<sub>6</sub> 八面体构型; 热重分析表明, 高温分解过程该化合物脱水转化为四硼酸镁 MgB<sub>4</sub>O<sub>7</sub>; 通过紫外可见漫反射法求得禁带宽度为 4.44 eV。

**关键词:** 镁硼酸盐; 含硼盐卤; 稀释成盐法; 结构; 热稳定性

中图分类号: O611.4 文献标识码: A 文章编号: 1001-4861(2015)02-0305-08

DOI: 10.11862/CJIC.2015.042

## Synthesis, Structure and Properties of a Magnesium Borate in Concentrated Boron-Bearing Salt Lake Brine by Dilution Method

PENG Jiao-Yu<sup>1,2,3</sup> LIN Feng<sup>1,2,3</sup> YANG Bo<sup>1</sup> WANG Li-Ping<sup>1,2,3</sup>

Dinnebier E. Robert<sup>4</sup> DONG Ya-Ping<sup>\*,1,2</sup> LI Wu<sup>1</sup>

(<sup>1</sup>Qinghai Institute of Salt Lakes, Chinese Academy of Sciences, Xining 810008, China)

(<sup>2</sup>University of Chinese Academy of Sciences, Beijing 100049, China)

(<sup>3</sup>Key Lab of Comprehensive and Highly Efficient Utilization of Salt Lake Resource,  
Chinese Academy of Science, Xining 810008, China)

(<sup>4</sup>Max-Planck Institute for Solid State Research, Stuttgart 70569, Germany)

**Abstract:** A new magnesium borate mineral, Mg[B<sub>6</sub>O<sub>7</sub>(OH)<sub>6</sub>]·5H<sub>2</sub>O was synthesized via dilution method from boron-bearing Na-K-Mg-Cl-SO<sub>4</sub> salt lakes. The crystal structure of the new phase was solved and refined using X-ray powder diffraction data and characterized with FTIR and Raman. Its asymmetric unit consists of one Mg atom, one B<sub>6</sub>O<sub>7</sub>(OH)<sub>6</sub> cluster and five H<sub>2</sub>O molecules. The Mg atom is 6-coordinated with six O atoms to form a MgO<sub>6</sub> octahedron. Thermal gravimetry (TG/DSC) was used to investigate the thermal behavior of the new compound. During the high temperature decomposition process the dehydrated product MgB<sub>4</sub>O<sub>7</sub> formed. The optical absorption characteristic of this new mineral was investigated by UV-Vis spectrometer and its energy gap  $E_g$  is about 4.44 eV.

**Keywords:** magnesium borate; boron-bearing salt lake; dilution method; structure; thermal behavior

收稿日期: 2015-07-13。收修稿日期: 2015-10-21。

国家青年科学基金(No.21501187), 青海省科技支撑项目(No.2013-G-138A), 青海省(应用)基础研究计划项目(NO. 2013-Z-705), 中国科学院仪器设备功能开发技术创新项目(No.Y410031012)资助。

\*通信联系人。E-mail: Dongyaping@hotmail.com

## 0 Introduction

Boron and its compounds are important inorganic salt products. Especially materials enriched in boron-10 are widely used in nuclear power, military equipment, and pharmaceuticals, etc, based on the property that boron-10 can absorb thermal neutrons. For example, the boric acid enriched in boron-10 used as neutron absorber in nuclear power can effectively ensure the nuclear reactor's safe operation<sup>[1]</sup>. Furthermore, boron minerals, owing to their high heat resistance, light weight, fire retardancy, nonlinear optics and anti-wear properties, can be widely applied in ceramics, metallurgy, building materials and electronic areas<sup>[2-5]</sup>. In recent years, with the increasing demand of boron products and the difficulty exploitation of low grade boron ores, boron exploitation from salt lake brine has become an important means to produce boron products<sup>[6]</sup>.

Lake Da Qaidam is one of the magnesium sulfate subtype salt lakes found on Qinghai Tibet Plateau in western China. The brine of which is abundant in sodium, potassium, magnesium, lithium and boron mineral resources. The main composition of the brine is Na-K-Mg-Cl-SO<sub>4</sub>. And the crystallization path about summer brine during evaporation was<sup>[7]</sup>:

halite  $\rightarrow$  halite+epsomite  $\rightarrow$  halite+epsomite + hexahydrite+sylvite  $\rightarrow$  halite+hexahydrite+sylvite + carnallite  $\rightarrow$  halite+hexahydrite+carnallite+bischofite.

When the brine evaporation path went into bischofite crystallization, the brine is rich in boron and lithium resources and can be used as raw material for the production of boron and lithium products. Gao and Li have investigated the chemical behavior of the borate during brine evaporation<sup>[8]</sup>. They found that the borate in this brine, in general, does not crystallize out but accumulates in the highly concentrated brine, in the form of polyborate anions of "tetraborate" by statistics. The supersolubility of boron enriched in the brine can reach up to 5.82% in B<sub>2</sub>O<sub>3</sub><sup>[9]</sup>. However, the fact will be exactly the opposite when diluting the boron-bearing highly concentrated brine with some water. Kinds of Mg-borate salts would

participate after diluting the brine for a period of time and the deposit salts changed with the dilution ratio of brine<sup>[10]</sup>. This phenomenon is quite different to crystallization by evaporation. Gao called it as "crystallization by dilution". The salts precipitated from diluted brine contain magnesium borate hydrate (MgO(B<sub>2</sub>O<sub>3</sub>)<sub>3</sub>·6H<sub>2</sub>O), macallisterite (Mg<sub>2</sub>[B<sub>6</sub>O<sub>7</sub>(OH)<sub>6</sub>]<sub>2</sub>·9H<sub>2</sub>O), admontite (MgO(B<sub>2</sub>O<sub>3</sub>)<sub>3</sub>·7H<sub>2</sub>O), hungchsaoite (Mg(H<sub>2</sub>O)<sub>5</sub>B<sub>4</sub>O<sub>5</sub>(OH)<sub>4</sub>·2H<sub>2</sub>O), kurnakovite (MgB<sub>3</sub>O<sub>3</sub>(OH)<sub>5</sub>(H<sub>2</sub>O)<sub>4</sub>·H<sub>2</sub>O) and inderite (MgB<sub>3</sub>O<sub>3</sub>(OH)<sub>5</sub>(H<sub>2</sub>O)<sub>4</sub>·H<sub>2</sub>O). The above results of "crystallization by dilution" indicate a possible economic extraction of boron resources from brine. Thus, we just call it as dilution method compared with traditional methods of acid precipitation and solvent extraction. During the dilution crystallization process, we found a new Mg-borate compound of Mg[B<sub>6</sub>O<sub>7</sub>(OH)<sub>6</sub>]<sub>2</sub>·5H<sub>2</sub>O from the highly concentrated brine. The present study aims to report the synthesis, structural characterization, optical and thermal properties of this new compound.

## 1 Experimental

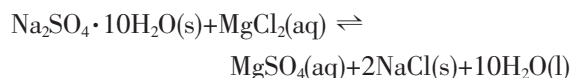
### 1.1 Materials and measurements

Mirabilite ores (Na<sub>2</sub>SO<sub>4</sub>·10H<sub>2</sub>O) were used to remove parts of Mg<sup>2+</sup> ion from brine for further evaporation purpose. The Raman spectra were recorded using a Raman spectrometer (ALMEGA-TM, Therm Nicolet, American) with the linearly polarized 532.0 nm line of a diode laser. The spectra were taken from 300 to 1 500 cm<sup>-1</sup> since the characteristic peaks of borate compounds were given in the range of 1 500~500 cm<sup>-1</sup><sup>[11]</sup>. The FTIR spectrum was obtained on a Fourier transform IR spectrometer (NEXUS, Therm Nicolet, American) with KBr pellet in the range of 400~4 000 cm<sup>-1</sup> at room temperature. The DSC and TG measurements were performed simultaneously using a scanning calorimeter (NETZSCH STA, 449F3) heating from 30 to 1 200 °C in nitrogen atmosphere with a constant heating rate of 5 °C·min<sup>-1</sup>. The Mg and B elements of the product was investigated by the inductive coupling plasma (ICP) spectrometer (Thermo, 6500) and the O element was measured by an Oxford series X-ray energy dispersion spectrometer

(EDS). The UV/Vis diffuse spectrum for  $\text{Mg}[\text{B}_6\text{O}_7(\text{OH})_6] \cdot 5\text{H}_2\text{O}$  was recorded with a Agilent Cary 5000 spectrophotometer in the range from 200 to 800 nm at room temperature.

## 1.2 Preparation of the concentrated boron-bearing brine

When the brine evaporation path went into bischofite crystallization, the boron content in brine is about 1.3% in  $\text{B}_2\text{O}_3$  which is too low to extract boron from brine by dilution method. Further evaporation is needed to concentrate the boron element. However, since the brine with saturated bischofite is extremely high-saline, viscous and hygroscopic and tends to absorb humidity from the air rather than drying. This brine can hardly be further concentrated by natural evaporation. In this study, according to the following reaction:



some mirabilite ores were added into the brine at 25 °C to react with the magnesium chloride generating magnesium sulfate and sodium chloride. Then the brine saturated with epsomite and halite can be easily further evaporated at room temperature. Therefore, the concentrated boron-bearing brine can be obtained by evaporation.

## 1.3 Synthesis of the magnesium borate of $\text{Mg}[\text{B}_6\text{O}_7(\text{OH})_6] \cdot 5\text{H}_2\text{O}$

The concentrated boron-bearing brine with boron content above 4%  $\text{B}_2\text{O}_3$  was used as materials to synthesize the new compound of  $\text{Mg}[\text{B}_6\text{O}_7(\text{OH})_6] \cdot 5\text{H}_2\text{O}$ . First, an amount of the concentrated brine was diluted with some water, the mass ratio of brine and water was 1:0.25. The solution was stirred for about 20 min each day at room temperature until the participation of solid phase, then aged and filtrated after a week. The sediment was washed by water and absolute alcohol, respectively, and dried in a vacuum drying oven for 24 h. The chemical composition of the obtained product was analyzed by titration.

## 1.4 X-ray powder diffraction crystallography

A laboratory powder diffractometer (X'Pert PRO, 2006 PANalytical,  $\text{Cu } K\alpha_1$ ), with a tube voltage and

current of 40 kV and 30 mA, was used to confirm the  $\text{Mg}[\text{B}_6\text{O}_7(\text{OH})_6] \cdot 5\text{H}_2\text{O}$  phase purity. The powder pattern was measured in the scanning range from 3.502 0° to 109.998 0°,  $2\theta$  with a scan step of 0.002° and at a fixed counting time of 16 s per step.

Owing to the difficulty to grow crystals suitable for single-crystal structure determination, the crystal structure was solved and refined using conventional X-ray powder diffraction techniques. The TOPAS 4.2 program suite<sup>[12]</sup> was used for indexing, obtaining structure solution, and refinement of the crystal structure model. The iterative least squares algorithm (LSI)<sup>[13]</sup> was employed to index the pattern, and resulted in a primitive monoclinic lattice. The unit cell and profile parameters were refined by a Pawley fit<sup>[14]</sup> using the fundamental parameters approach<sup>[15]</sup>. The background was modelled by a Chebychev polynomial of 10th order.

## 2 Results and discussion

### 2.1 Evaporation crystallization path

The brine evolution during evaporation was represented graphically on the metastable phase diagram of  $\text{Na}^+$ ,  $\text{K}^+$ ,  $\text{Mg}^{2+}/\text{Cl}$ ,  $\text{SO}_4^{2-}/\text{H}_2\text{O}$  at 25 °C<sup>[16]</sup> (Fig.1). Its composition was listed in Table 1. In Fig. 1,  $\text{DL}_0$  was the residue bittern of Da Qaidam salt lake during evaporation and its system was located in the bischofite phase. After removing parts of  $\text{Mg}^{2+}$  ion by adding some mirabilite ores, the brine system “ $\text{DL}_1$ ” gone into the epsomite region and is easy to concentrate by evaporation. When the crystallization path

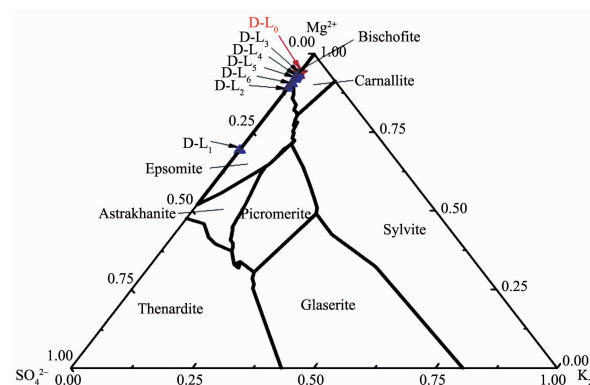


Fig.1 Crystallization path of brine  $\text{DL}_1$  at metastable diagram of  $\text{Na}^+$ ,  $\text{K}^+$ ,  $\text{Mg}^{2+}/\text{Cl}$ ,  $\text{SO}_4^{2-}/\text{H}_2\text{O}$  at 25 °C

**Table 1** Evolution of major ion concentrations during evaporation at ambient temperature

Brine	Concentration / %						
	Na <sup>+</sup>	Mg <sup>2+</sup>	K <sup>+</sup>	B <sub>2</sub> O <sub>3</sub>	Cl <sup>-</sup>	SO <sub>4</sub> <sup>2-</sup>	Li <sup>+</sup>
DL <sub>0</sub>	0.107±0.003	8.863±0.086	0.048±0.001	1.284±0.009	24.472±0.160	2.268±0.004	0.144 0±0.003
DL <sub>1</sub>	2.577±0.125	5.515±0.031	0.037±0.001	0.970±0.005	13.020±0.498	9.638±0.017	0.104 0±0.001
DL <sub>2</sub>	0.122±0.006	8.022±0.051	0.084±0.001	2.187±0.012	20.797±0.861	3.832±0.007	0.209 8±0.002
DL <sub>3</sub>	-0.072±0.02	8.782±0.054	0.059±0.001	2.825±0.020	23.665±0.158	2.474±0.004	0.267 6±0.006
DL <sub>4</sub>	0.424±0.017	8.869±0.060	0.063±0.001	3.244±0.021	23.592±0.181	2.806±0.005	0.142 8±0.005
DL <sub>5</sub>	-0.041±0.001	8.773±0.059	0.063±0.001	4.352±0.039	22.671±0.145	3.018±0.005	0.298 4±0.004
DL <sub>6</sub>	0.055±0.003	8.636±0.055	0.087±0.001	5.163±0.028	21.96 0±1.023	3.538±0.006	0.360 9±0.003

evolved from epsomite (DL<sub>1</sub>) to bischofite (DL<sub>3</sub>), the boron content in brine was concentrated to about 3% in B<sub>2</sub>O<sub>3</sub> (Table 1). This brine can be used to extract boron by dilution method. But, for the synthesis of the new compound, it will be further evaporated until the boron content is above 4% B<sub>2</sub>O<sub>3</sub>. Therefore, the concentrated boron-bearing brine DL<sub>5</sub> or DL<sub>6</sub> obtained by evaporation were used as materials for the synthesis of the new compound.

## 2.2 XRD pattern and crystal structure characterization

Fig.2 shows the X-ray diffraction pattern of Mg[B<sub>6</sub>O<sub>7</sub>(OH)<sub>6</sub>]·5H<sub>2</sub>O and the results of the Rietveld refinement<sup>[17]</sup>. The refined structural parameters are presented in Table 2. The obtained product was phase pure according to the X-ray powder diffraction. The chemical elements analyzed by titration and the crystal water measured by TG are shown in Table 3. The measured composition values fit well with the given formula.

In Fig.2, the X-ray diffraction pattern shows remarkable similarity to the pattern of Ni[B<sub>6</sub>O<sub>7</sub>(OH)<sub>6</sub>]·5H<sub>2</sub>O<sup>[18]</sup>. For comparability reasons, the standard crystallographic space group setting *P2<sub>1</sub>/c* of Ni[B<sub>6</sub>O<sub>7</sub>(OH)<sub>6</sub>]·5H<sub>2</sub>O was kept for Mg[B<sub>6</sub>O<sub>7</sub>(OH)<sub>6</sub>]·5H<sub>2</sub>O (Element analysis: Mg 6.38%, B 15.99%, O 73.20%) leading to lattice parameters of *a*=0.898 87(3) nm, *b*=2.179 35(7) nm, *c*=0.720 79(2) nm, *γ*=99.8759(6)°, and *V*=1.391 07(8) nm<sup>3</sup>.

In the crystal structure of Mg[B<sub>6</sub>O<sub>7</sub>(OH)<sub>6</sub>]·5H<sub>2</sub>O (Fig.3), the asymmetric unit consists of one Mg atom, one B<sub>6</sub>O<sub>7</sub>(OH)<sub>6</sub> cluster and five H<sub>2</sub>O molecules. The B atoms are in both 3- and 4-coordinated environments forming BO<sub>3</sub> triangles and BO<sub>4</sub> tetrahedra. Three BO<sub>3</sub> and three BO<sub>4</sub> units are connected by sharing a common O atom to form B<sub>6</sub>O<sub>7</sub>(OH)<sub>6</sub>. The Mg atom is 6-coordinated with six O atoms to form a MgO<sub>6</sub> octahedron. In each units MgO<sub>6</sub> octahedron, the Mg atom shares two common O atoms with one B<sub>6</sub>O<sub>7</sub>(OH)<sub>6</sub> cluster and four common O atoms with four H<sub>2</sub>O

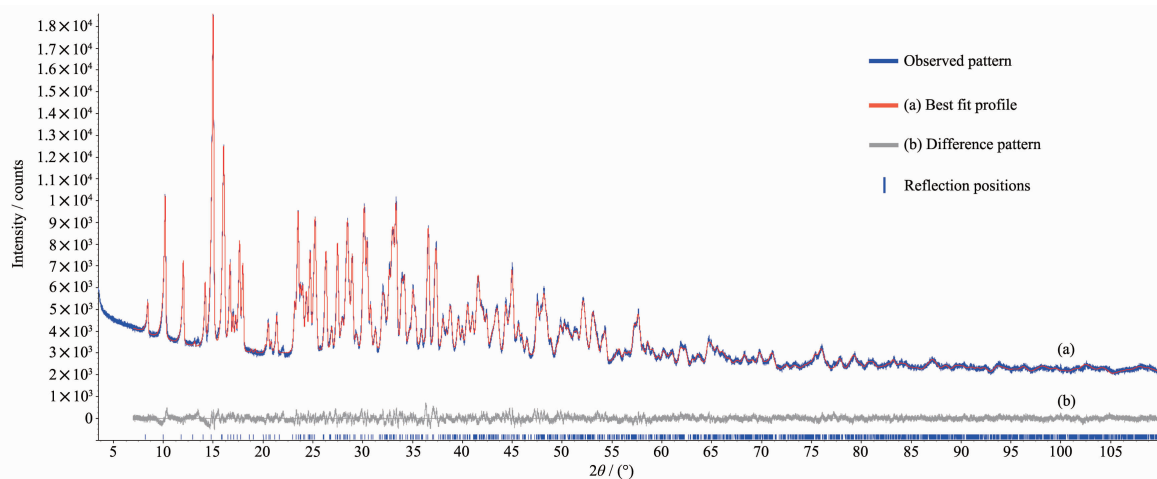


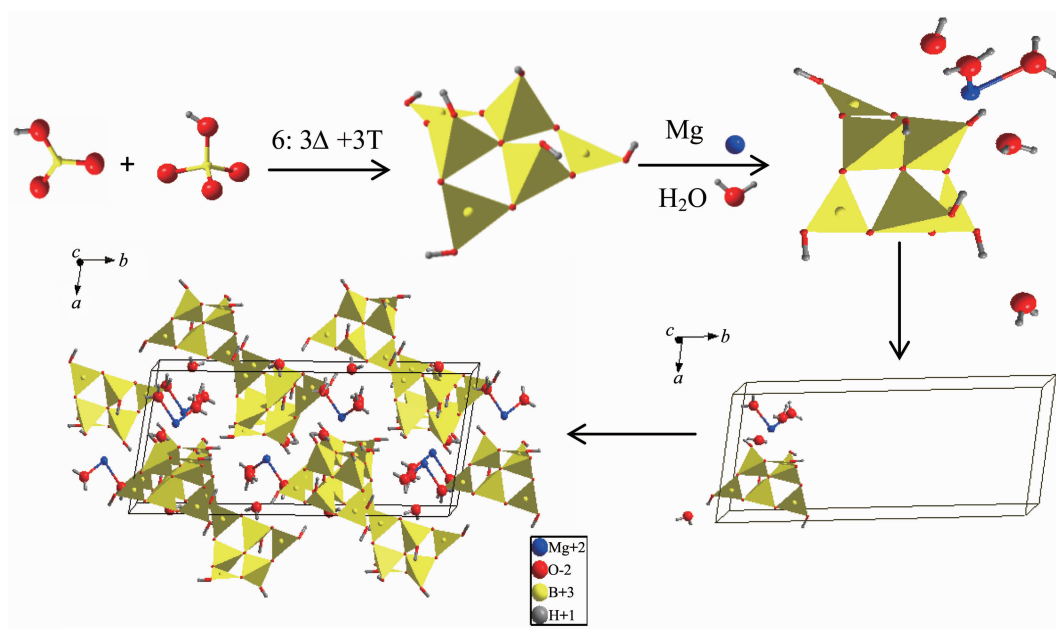
Fig.2 X-ray diffraction pattern of Mg[B<sub>6</sub>O<sub>7</sub>(OH)<sub>6</sub>]·5H<sub>2</sub>O and results of the rietveld refinement

**Table 2** Crystallographic and rietveld refinement data for  $\text{Mg}[\text{B}_6\text{O}_7(\text{OH})_6] \cdot 5\text{H}_2\text{O}$ 

Empirical formula	$\text{Mg}[\text{B}_6\text{O}_7(\text{OH})_6] \cdot 5\text{H}_2\text{O}$	$a / \text{nm}$	0.898 87(3)
Compound	Magnesium Borate	$b / \text{nm}$	2.179 35(7)
Formula weight	393.28	$c / \text{nm}$	0.720 79(2)
Starting angle $2\theta / (^\circ)$	3.5	$\gamma / (^\circ)$	99.875 9(6)
Final angle $2\theta / (^\circ)$	110	Volume / $\text{nm}^3$	1.391 07(8)
Data collection / (s per step)	26.67	$R_{\text{Bragg}} / \%$	1.67
Temperature / $^\circ\text{C}$	25	$R_{\text{exp}} / \%$	2.62
Crystal system	Monoclinic	$R_p / \%$	4.26
Space group	$P2_1/c$	$R_{\text{wp}} / \%$	5.53
Z	4	No. of variables	100

**Table 3** Titration analysis of the  $\text{Mg}[\text{B}_6\text{O}_7(\text{OH})_6] \cdot 5\text{H}_2\text{O}$  phase

	MgO	$\text{B}_2\text{O}_3$	$\text{H}_2\text{O}$
Theoretical	10.25	53.11	36.65
Experimental	10.33	52.85	36.84

**Fig.3** Crystal structure of the  $\text{Mg}[\text{B}_6\text{O}_7(\text{OH})_6] \cdot 5\text{H}_2\text{O}$  compound

forming a 3D  $\text{Mg}(\text{H}_2\text{O})_4\text{B}_6\text{O}_7(\text{OH})_6$  framework. Furthermore, the last one  $\text{H}_2\text{O}$  connects with the  $\text{Mg}(\text{H}_2\text{O})_4\text{B}_6\text{O}_7(\text{OH})_6$  framework to form the whole structure of  $\text{Mg}[\text{B}_6\text{O}_7(\text{OH})_6] \cdot 5\text{H}_2\text{O}$ .

In the  $\text{B}_6\text{O}_7(\text{OH})_6$  cluster, the B-O distances of  $\text{BO}_3$  triangles are in the range of 0.135 7~0.138 5 nm (average 0.136 8 nm), and the B-O distances of  $\text{BO}_4$  tetrahedra are in the range of 0.143 8~0.152 4 nm (average 0.147 7 nm). The O-B-O angles of the  $\text{BO}_3$  triangles and the  $\text{BO}_4$  tetrahedra are in the range of

115.018°~122.712° and 107.226°~111.398°, respectively. The Mg-O distances are in the range of 0.203 5~0.213 7 nm. The bond distances and angles of the compound are in agreement with other borate compounds reported previously<sup>[19-21]</sup>.

### 2.3 FTIR and raman spectroscopy

Fig.4 and Fig.5 show the FT-IR and Raman spectra of  $\text{Mg}[\text{B}_6\text{O}_7(\text{OH})_6] \cdot 5\text{H}_2\text{O}$ , respectively. In the FT-IR spectrum, the bands at high wavenumbers of 3 200~3 600  $\text{cm}^{-1}$  belonged to stretching of hydroxyl



( $\nu(\text{O-H})$ ); and the peak at  $1\,663\text{ cm}^{-1}$  corresponded to bending of H-O-H. According to literatures<sup>[11,22]</sup>, The bands at  $1\,420$ ,  $1\,350\text{ cm}^{-1}$  were assigned to asymmetric stretching of the three-coordinate boron ( $\nu_{\text{as}}(\text{B}_{(3)}\text{-O})$ ). The bending of B-O-H was observed at band of  $1\,253\text{ cm}^{-1}$ . The peaks between  $1\,174$  and  $1\,053\text{ cm}^{-1}$  belonged to asymmetric stretching of four-coordinated boron ( $\nu_{\text{as}}(\text{B}_{(4)}\text{-O})$ ). The symmetric stretching of  $\text{B}_{(3)}\text{-O}$  and  $\text{B}_{(4)}\text{-O}$  was observed in the range of  $807\sim 944\text{ cm}^{-1}$ . And the band around  $682$  was out-of-plane bending of  $\text{B}_{(3)}\text{-O}$ .

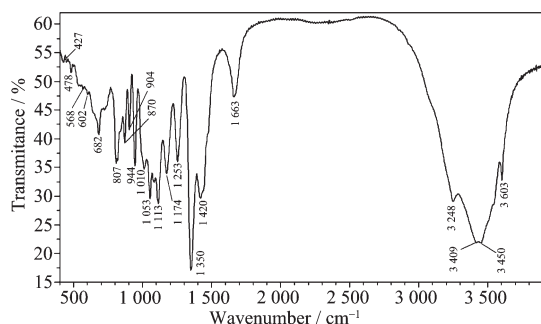


Fig.4 FT-IR spectrum of the  $\text{Mg}[\text{B}_6\text{O}_7(\text{OH})_6]\cdot 5\text{H}_2\text{O}$  compound

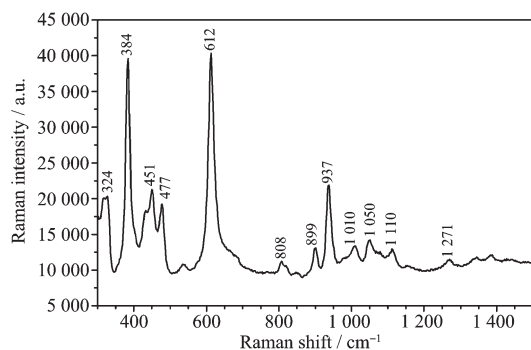


Fig.5 Raman spectrum of the  $\text{Mg}[\text{B}_6\text{O}_7(\text{OH})_6]\cdot 5\text{H}_2\text{O}$  compound

In the Raman spectrum, based on the assignment of borates<sup>[22-24]</sup>, weak bands in the region of  $1\,200\sim 1\,400\text{ cm}^{-1}$  and  $1\,110\sim 1\,000\text{ cm}^{-1}$  were asymmetric stretching of the three-coordinate boron ( $\nu_{\text{as}}(\text{B}_{(3)}\text{-O})$ ) and four-coordinate boron ( $\nu_{\text{as}}(\text{B}_{(4)}\text{-O})$ ), respectively. The band at  $937\text{ cm}^{-1}$  was assigned to symmetric stretching of the three-coordinate boron ( $\nu_{\text{s}}(\text{B}_{(3)}\text{-O})$ ); and the bands around  $899$ ,  $808\text{ cm}^{-1}$  were  $\nu_{\text{s}}(\text{B}_{(4)}\text{-O})$ . Generally, the bands in the range of  $610\sim 650\text{ cm}^{-1}$  were associated with the symmetric pulse vibration of tetraborate anion or hexaborate anion<sup>[22]</sup>. In this study, the strong

band at  $612\text{ cm}^{-1}$  belonged to the characteristic peaks of  $\nu_{\text{p}}(\text{B}_6\text{O}_7(\text{OH})_6^{2-})$ . Besides, the peaks at and below  $477\text{ cm}^{-1}$  were assigned to bending of four-coordinate boron ( $\delta(\text{B}_{(4)}\text{-O})$ ).

### 3.4 Thermal analysis

TG and DSC analyses of the  $\text{Mg}[\text{B}_6\text{O}_7(\text{OH})_6]\cdot 5\text{H}_2\text{O}$  phase are shown in Fig.6. Three endothermic peaks ( $151$ ,  $211$  and  $994\text{ }^\circ\text{C}$ ) and one exothermic peak ( $694\text{ }^\circ\text{C}$ ) occurred in the DSC curve. In the first step, the weight loss is about 20% which was similar to the theoretical values of five water molecules weight of 22.90%, indicating there were five water molecules in the compound. In the second step, the weight loss was about 17%, which can be regarded as the weight of six hydroxyls (theoretical value of 13.75%) and the remaining water. The above total weight loss is about 37% corresponding to the weight of five water molecules and six hydroxyl (theoretical values of 36.65%) in the compound. In the third step, the structure of the compound was changed after removing five water molecules and six hydroxyl. The fourth step indicates the melting point of the calcined crystals.

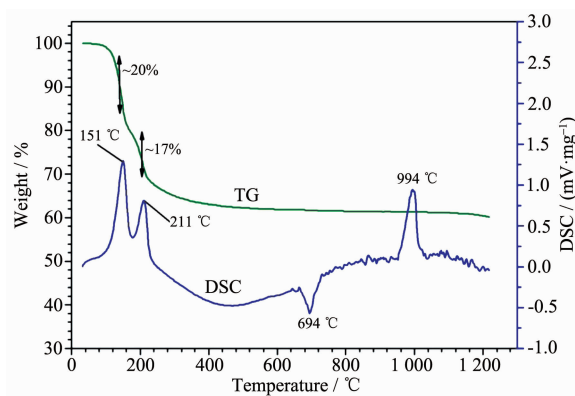


Fig.6 TG and DSC analyses of the  $\text{Mg}[\text{B}_6\text{O}_7(\text{OH})_6]\cdot 5\text{H}_2\text{O}$  compound

To study the thermal decomposition behavior, the dehydrated products calcined at  $400$ ,  $800$  and  $1\,000\text{ }^\circ\text{C}$  were confirmed by XRD analysis (Fig.7). Before XRD analysis, the dehydrated product calcined at  $800\text{ }^\circ\text{C}$  was treated with methanol solution by esterification reaction to remove  $\text{B}_2\text{O}_3$  which occurred together with the dehydrated product during calcination process. In Fig.7, the exothermic peak around  $694\text{ }^\circ\text{C}$  marked the transition of the dehydrated amorphous product to

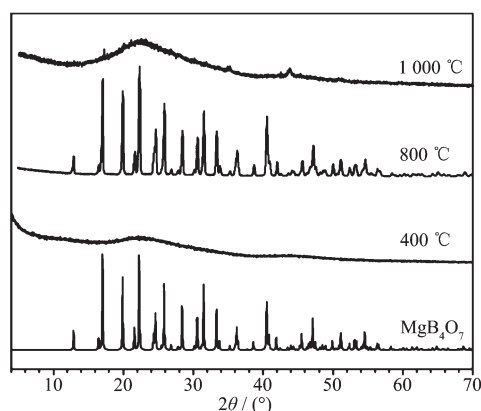
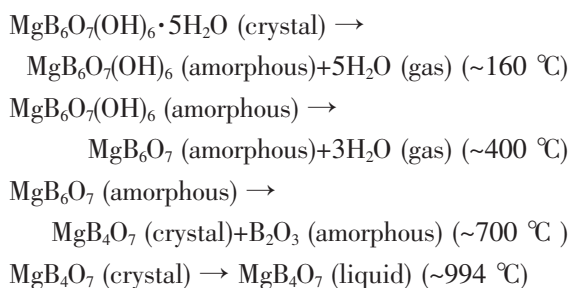


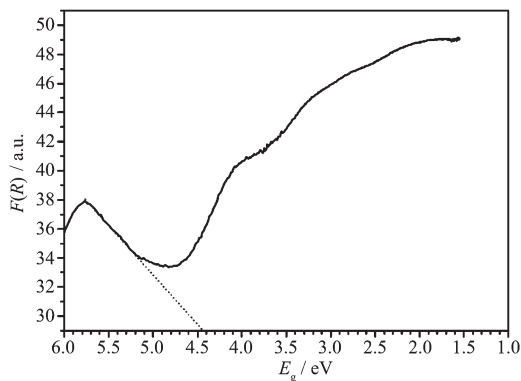
Fig.7 XRD patterns of dehydrated products

$\text{MgB}_4\text{O}_7$  (PDF card: 00-01-0927). While the calcined temperature went up to about 1 000 °C, the  $\text{MgB}_4\text{O}_7$  crystal began to melt and stuck in the alumina crucible during cooling process. Therefore, a whole decomposition process is presented by the following chemical reactions:



### 3.4 Results of optical measurements

Fig.8 shows the absorption spectrum of  $\text{Mg}[\text{B}_6\text{O}_7(\text{OH})_6] \cdot 5\text{H}_2\text{O}$  compound. The absorption data were calculated from the following Kubelka-Munk function:  $F(R) = (1-R)^2/(2R)$ , where  $R$  is the reflectance. The energy gap  $E_g$  was calculated by the function:  $E_g = 1240/\lambda$ , where  $\lambda$  is the wavelength. In Fig.8, the energy gap

Fig.8 Optical absorption spectra of  $\text{Mg}[\text{B}_6\text{O}_7(\text{OH})_6] \cdot 5\text{H}_2\text{O}$  compound

$E_g$  of  $\text{Mg}[\text{B}_6\text{O}_7(\text{OH})_6] \cdot 5\text{H}_2\text{O}$  compound determined from extrapolation of high energy part of absorption spectra is about 4.44 eV.

### 3 Conclusions

A new magnesium borate mineral,  $\text{Mg}[\text{B}_6\text{O}_7(\text{OH})_6] \cdot 5\text{H}_2\text{O}$  has been synthesized by dilution method from boron-bearing salt lakes for the first time at room temperature. The low reaction temperature used in this study provides a green chemistry approach for the synthesis of magnesium borate. The dilution crystallization method also provides a possible economic extraction of boron resources from salt lake brine. The crystal structure of this new compound was solved by laboratory X-ray powder diffraction data. The compound crystallizes in the monoclinic space group  $P2_1/c$ . Its crystal structure consists of infinite chains of  $\text{B}_6\text{O}_7(\text{OH})_6$  clusters, intercalated by  $\text{MgO}_6$  and  $\text{H}_2\text{O}$  molecules, forming a 3D framework. The vibrational spectroscopy of FTIR and Raman reveals the presence of  $\text{BO}_3$  triangles,  $\text{BO}_4$  tetrahedra, water  $\text{H}_2\text{O}$  and the characteristic  $\text{B}_6\text{O}_7(\text{OH})_6^{2-}$  anion in the compound, which further verifies the structural characterization by X-ray powder diffraction. The thermal analysis (TG and DSC) showed that there were at least four phases occurred during decomposition process. The thermal behavior goes through the transformation from amorphous to crystal phase of  $\text{MgB}_4\text{O}_7$ . The optical measurement found that the energy gap of the new magnesium borate is about 4.44 eV.

### References:

- [1] XU Jiao(许姣), ZHANG Wei-Jiang(张卫江). *Nucl. Sci. Eng.* (核科学与工程), **2012**, **32**:238-243
- [2] Mhareb M H A, Hashima S, Ghoshal S K, et al. *Opt. Mater.*, **2014**, **37**:391-397
- [3] Chen S H, Zhang D F, Sun G. *Mater. Lett.*, **2014**, **121**:206-208
- [4] Li Y, Fan Z, Lu J G, et al. *Chem. Mater.*, **2004**, **16**:2512-2514
- [5] Zhu W, Li G, Zhang Q, et al. *Powder Technol.*, **2010**, **203**:265-271
- [6] Xu L, Liu Y Q, Hu H P, et al. *Desalination*, **2012**, **294**:1-7
- [7] GAO Shi-Yang(高世扬), Song Peng-Sheng(宋彭生), XIA

- Shu-Ping(夏树屏), et al. *Proceedings of Salt Lake Chemistry: Vol.2*(盐湖化学论文集:第 2 册). Qinghai: Qinghai Bureau Printing House, **1995**:18-32
- [8] GAO Shi-Yang(高世扬), LI Guo-Ying(李国英). *Chem. J. Chinese Universities*(高等学校化学学报), **1982**,**3**:141-148
- [9] GAO Shi-Yang(高世扬), FU Ting-Jin(符廷进), WANG Jian-Zhong(王建中). *Chinese J. Inorg. Chem.*(无机化学学报), **1985**,**1**:97-102
- [10] GAO Shi-Yang(高世扬), XU Kai-Fen(许开芬), LI Gang(李刚), et al. *Acta Chim. Sinica*(化学学报), **1986**,**44**:1229-1233
- [11] Jia Y Z, Gao S Y, Xia S P, et al. *Spectrochim. Acta A*, **2000**,**56**:1291-1297
- [12] TOPAS 4.2, Bruker AXS Inc.: Madison, Wisconsin, USA, **2009**.
- [13] Coelho A A. *J. Appl. Crystallogr.*, **2003**,**36**:86-95
- [14] Pawley G S. *J. Appl. Crystallogr.*, **1981**,**14**:357-361
- [15] Cheary R W, Coelho A A, Cline J P. *J. Res. Nat. Inst. Stand. Technol.*, **2004**,**109**:1-25
- [16] JIN Zuo-Mei(金作美), XIAO Xian-Zhi(肖显志), LIANG Shi-Mei(梁式梅). *Acta Chim. Sinica*(化学学报), **1980**,**38**:313-321
- [17] Rietveld H M. *J. Appl. Crystallogr.*, **1969**,**2**:65-71
- [18] Silin E Y, Ievinsh A F. *Z. Kristallogr.*, **1977**,**22**:505-509
- [19] Liu Z H, Li L Q, Zhang W J. *Inorg. Chem.*, **2006**,**45**:1430-1432
- [20] Wu H Q, Wei Q, He H, et al. *Inorg. Chem. Commun.*, **2014**,**46**:69-72
- [21] Sohr G, Falkowski V, Huppertz H. *J. Solid State Chem.*, **2015**,**225**:114-119
- [22] Li J, Xia S P, Gao S Y. *Spectrochim. Acta*, **1995**,**51A**:519-532
- [23] Liu Z H, Gao B, Hu M C, et al. *Spectrochim. Acta Part A*, **2003**,**59**:2341-2345
- [24] JIA Yong-Zhong(贾永忠), GAO Shi-Yang(高世扬), XIA Shu-Ping(夏树屏), et al. *Chem. J. Chinese Universities*(高等学校化学学报), **2001**,**22**:199-103